

# Dielectric Relaxation of Linear and Cross-Linked Polyurethane

Taco Nicolai

Polymères, Colloïdes, Interfaces, UMR CNRS, Université du Maine, 72085 Le Mans Cedex 9, France

Received June 11, 2001

**ABSTRACT:** The dielectric relaxation is studied of linear and cross-linked polyurethane based on linear and three-armed star poly(propylene oxide), also called poly(propylene glycol). The dielectric relaxation of polyurethane melts and gels is indistinguishable if the density of urethane links is the same. The introduction of urethane links slows down the segmental relaxation of a number of segments adjacent to the links. The influence is much stronger on the dielectric relaxation than on the relaxation of the shear modulus. The relaxation of the end-to-end vector of the PPO precursors is not much influenced by end-linking at least as long as they are not strongly entangled.

## Introduction

In the past the mechanic and dielectric relaxation of linear and three-armed star poly(propylene oxide) (PPO) have been studied extensively.<sup>1–10</sup> With mechanical spectroscopy (MS) one observes close to the glass transition temperature ( $T_g$ ) the local segmental relaxation ( $\alpha$ -relaxation) and at higher temperatures the conformational relaxation which is well described in terms of a superposition of normal modes following the Rouse model.<sup>10</sup> The effect of entanglements becomes visible if the spanning molar mass ( $M_s$ ) is larger than 4 kg/mol.  $M_s$  is the total mass for linear PPO or the mass of two arms for star PPO. With dielectric spectroscopy (DS) four relaxation modes are observed which are in order of increasing frequency: the relaxation of the end-to-end vector, the  $\alpha$ -relaxation, the relaxation of trace water, and the  $\beta$ -relaxation. The  $\alpha$ -relaxation observed in DS has the same temperature dependence as the one observed in MS but is systematically slower by a factor of 10. Generally, conformational relaxation cannot be observed in DS. However, PPO is one of very few polymers that have a dipole moment parallel to the chain backbone.<sup>3</sup> Therefore, the end-to-end vector relaxation can be observed in DS and was found to be consistent with the Rouse model.<sup>10</sup>

End-linking of PPO leads to dramatic changes of the mechanical properties. In the case of star PPO, gels are formed while if linear PPO is used entangled melts are formed. In the past few years the dynamic mechanical properties of polyurethane (PU) produced by polycondensation of both linear and star PPO and a diisocyanate<sup>11–14</sup> have been extensively investigated. For one star PPO the system was studied in detail as a function of the connectivity extent either in situ at different reaction extents<sup>12</sup> or at complete reaction by varying the ratio,  $r$ , of isocyanate groups to hydroxyl groups.<sup>13,14</sup> The effect of varying molar mass of the precursors was investigated for fully end-linked systems, i.e.,  $r = 1$  and after complete reaction.<sup>11</sup> The effect of end-linking on the glass transition temperature is determined by the effect of the fraction of urethane links and is similar for linear and cross-linked PU.

Here an investigation is reported of the dynamics of fully end-linked linear and star PPO using DS. For one sample the mechanical and dielectric relaxation was studied at different degrees of end-linking. DS is complementary to MS for a number of reasons. First, the dynamical range covered by DS is much larger than

for MS and allows one to study the local segmental ( $\alpha$ -) relaxation over a larger temperature range. Second, the sub-glass ( $\beta$ -) relaxation could not be measured in MS but is clearly visible in DS. Finally, in the special case of end-linked PPO, DS probes the end-to-end vector fluctuations between the urethane links. Contrary to MS, relaxation processes over larger distances are not seen in DS because the direction of the dipole moment is inverted at each urethane link.

Earlier this property was used to compare the mobility of cross-links in a PU gel with that of entanglements in a PU melt.<sup>15</sup> We used star and linear PPO with spanning molar mass equal to the entanglement molar mass. In this way DS probes the relaxation of the end-to-end vector between of chain segments of the same length either between covalent cross-links or between entanglements. The dielectric relaxation of the two systems was found to be identical, from which we concluded that the mobility of covalent cross-links is the same as that of entanglements.

However, the loss peak of the dielectric permittivity ( $\epsilon''$ ) at higher frequencies was broader after end-linking. Since a large PPO precursor was used in this study, the relative contribution of the urethane links to the total dipole moment is small. Thus, it is clearly the dynamics of the PPO segments that are modified by end-linking. On the other hand, it was not clear whether it is the component of the dipole moment parallel or perpendicular to the polymer backbone which is modified.

To resolve this point, we studied the dielectric relaxation of linear poly(propylene sulfide) (PPS) end-linked with a diisocyanate to form an entangled melt of polycarbamothioate (PCT).<sup>16</sup> The difference between PPO and PPS is that all oxygen atoms in PPO are replaced by sulfur in PPS. Therefore, hydrogen bonding which is important in PPO is insignificant in PPS. Nevertheless, the dynamical properties of PPS and PPO are very similar.<sup>17</sup> The main difference is that the glass transition temperature of PPO shows only a weak finite size effect on  $T_g$  due to hydrogen bonding of the chain ends, while PPS shows the characteristic decrease of  $T_g$  at lower molar mass observed for most polymers. Another consequence of the replacement of oxygen by sulfur is that the component of the dipole moment parallel to the polymer backbone becomes insignificant. Consequently, the relaxation of the end-to-end vector fluctuations of PPS is not seen in DS.

**Table 1. Number-Average Molar Mass and Polydispersity Index of the Linear and Star Precursors; Glass Transition Temperatures of the Fully End-Linked Samples**

|       | $M_n$ (g/mol) | $M_w/M_n$ | $T_g$ (K) | $T_{gv}$ |
|-------|---------------|-----------|-----------|----------|
| D425  | 426           | 1.06      | 245       | 244      |
| D1000 | 1010          | 1.04      | 222       | 219      |
| D2200 | 2040          | 1.08      | 215       | 212      |
| D4200 | 4060          | 1.2       | 210       | 208      |
| D8000 | 7400          | 1.2       | 210       | 205      |
| T720  | 720           | 1.08      | 261       | 257      |
| T2500 | 2590          | 1.08      | 221       | 214      |
| T6300 | 6200          | 1.2       | 215       | 208      |
| T8000 | 7600          | 1.2       | 210       | 206      |

The main conclusion of the study of end-linked PPS is that the segmental relaxation of a number of PPS segments is slowed down by the presence of carbamothioate links. As a consequence, the spectrum of the loss dielectric permittivity ( $\epsilon''$ ) shows an additional loss peak due to the segmental relaxation of the modified PPS segments ( $\alpha'$ -relaxation). The  $\alpha'$ -relaxation is slower than the segmental relaxation of the nonmodified PPS segments ( $\alpha$ -relaxation), but the two loss peaks overlap strongly so that it is difficult to distinguish them. Only if the amplitude of the two modes is about the same can they clearly be identified. The relative amplitude of the two modes depends on the density of the carbamothioate links, i.e., the molar mass of the precursor PPS. If low molar mass PPS is used, the  $\alpha'$ -relaxation dominates while if high molar mass PPS is used, the  $\alpha$ -relaxation dominates. The amplitudes of the two modes are the same if the molar mass is about 1.5 kg/mol.

The aim of the present work was to investigate the dielectric relaxation of linear and cross-linked polyurethane based on PPO with a range of different molar masses.

## Experimental Section

Polyurethanes were formed by polycondensation of PPO triols and diols with hexamethylene diisocyanate (HMDI) (Aldrich). The purity of HMDI was found from NMR to be better than 95%. The polyols used in this study have been characterized by size exclusion chromatography (SEC) using both refractive index and UV absorption detection. The number-averaged molar mass ( $M_n$ ) and the polydispersity index ( $M_w/M_n$ ) are summarized in Table 1. Water was removed as far as possible by submitting the polyols to high vacuum.

To obtain fully end-linked systems, the ratio of isocyanate groups to hydroxyl groups,  $r = [\text{NCO}]/[\text{OH}]$ , needs to be unity. The amount of HMDI needed to obtain  $r = 1$  was calculated on the basis of the hydroxyl content of the samples.  $2 \times 10^{-3}$  g of dibutyl tin dilaurate catalyst was added for every gram of HMDI. After mixing and complete homogenization of the reaction components, the samples were cured at 40 °C until complete consumption of the isocyanate groups.

Ideally complete end-linking leads to a three-dimensional network in the case of triol and an entangled melt of extremely long linear chains in the case of diol. In practice, however, the gel contains defects, and the linear polyurethane chains are not very long. The average number of diols per polyurethane chain decreases with the length of the diol but is always more than 10; see ref 11.

**Dielectric Spectroscopy.** Measurements of the complex dielectric permittivity were made with broad-band dielectric spectroscopy equipment from Novocontrol GmbH. Measurements were made in the frequency range from  $10^{-1}$  up to  $10^6$  Hz. The samples were kept between two gold-plated stainless steel plates of 20 or 40 mm in diameter with a gap varying between 30 and 500  $\mu\text{m}$ . The sample cell was placed in a cryostat, and the sample temperature was regulated with an

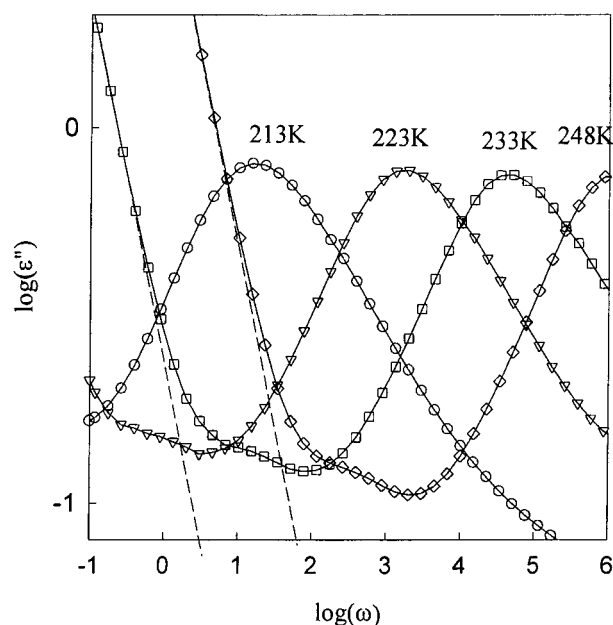


**Figure 1.** Double-logarithmic representation of the dielectric loss spectra of end-linked linear PPO (D8200) at different temperatures indicated in the figure. The dashed lines indicate the contribution of the conductivity due to charged impurities

accuracy of  $\pm 0.1$  K and measured with a PT100 sensor in the lower plate of the sample capacitor.

**Mechanic Spectroscopy.** Dynamic shear measurements were made on a Rheometrics RDA II dynamic spectrometer using parallel-plate geometry. The so-called hold mode was used where the gap is corrected for temperature variations of the sample volume. The plate size and the imposed deformation were adjusted to obtain an accurate torque response while remaining in the linear regime. The shear modulus could be measured in the range  $10$ – $10^9$  Pa. We were able to measure very large moduli by using a relatively large sample thickness (2–2.5 mm) in combination with a small plate size. The range of frequencies,  $f$ , used was  $2 \times 10^{-3}$ –20 Hz. Temperatures were measured using a thermocouple close to the lower plate. The temperature was stable within  $\pm 0.2$  K over the whole range used in this study.

Glass transition temperatures were determined using differential scanning calorimetry (DSC). The samples were cooled rapidly to 170 K and then heated at a rate of 10 deg/min. Values of  $T_g$  were taken as the midpoint of the transition. The reproducibility is  $\pm 2$  K.

## Results and Discussion

Glass transition temperatures of the polyurethanes used in this study are summarized in Table 1. As was discussed in ref 11, the introduction of urethane links increases the glass transition temperature. The frequency dependence of the dielectric response was measured for fully end-linked linear and star PPO with different molar masses over a range of temperatures. Below  $T_g$  one observes the relaxation of trace water and the  $\beta$ -relaxation. These relaxation processes are not much influenced by end-linking and have the same activation energy as before end-linking. I will not discuss the sub-glass relaxation in more detail here, but see ref 16 for a discussion of the effect of end-linking on the  $\beta$ -relaxation of PPS. Close to and above  $T_g$  the segmental relaxation is observed, and for the larger precursors one observes in addition the conformational relaxation (see Figure 1). The upturn at low frequencies is caused by the conductivity due to charged impurities. The contribution of the conductivity is inversely pro-

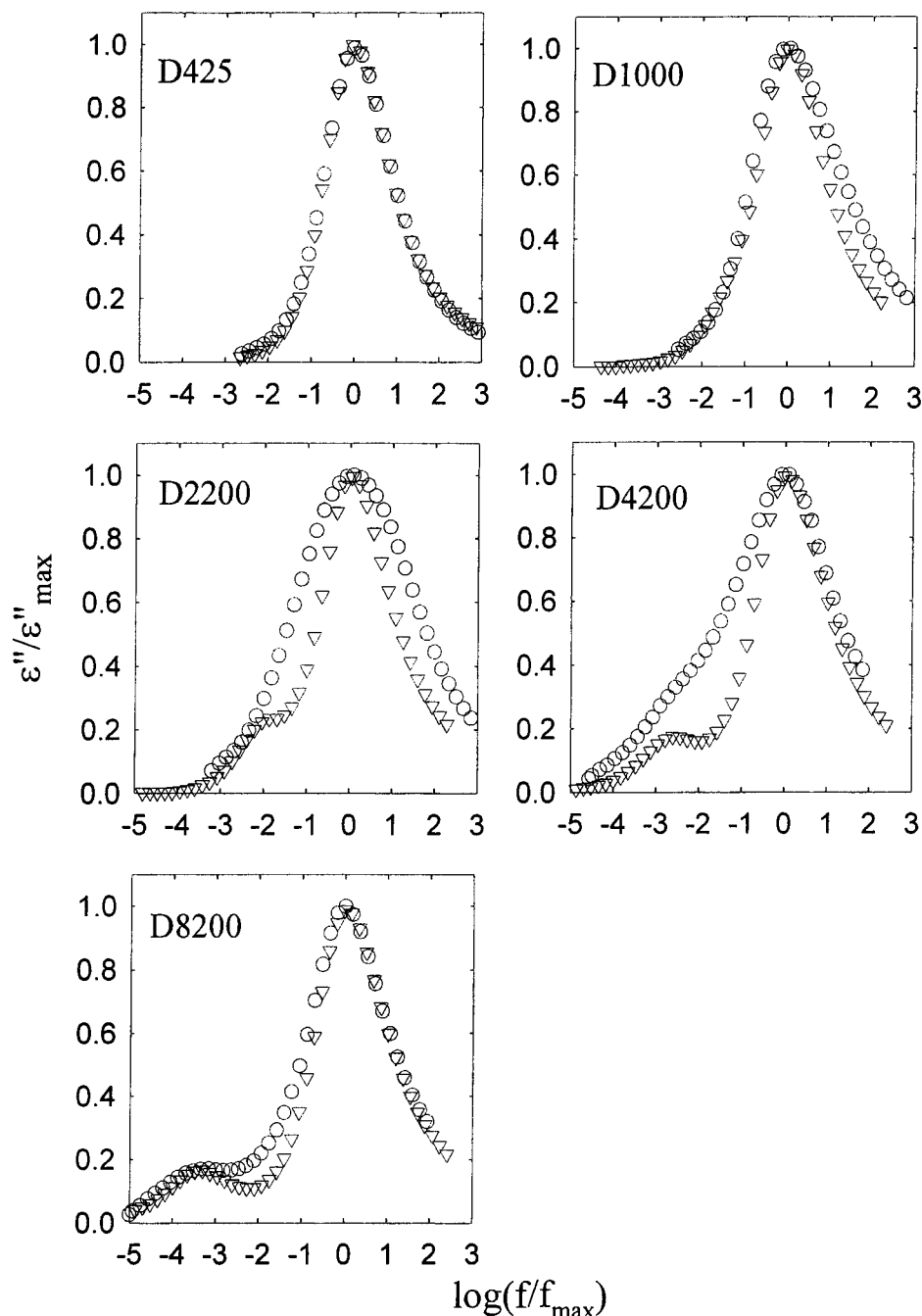


**Figure 2.** Comparison of the normalized dielectric loss spectra of linear PPO before (triangles) and after (circles) end-linking.

portional to the frequency (see dashed lines in Figure 1) and overlaps with the conformational relaxation of polyurethane based on large precursors. The extent of the overlap increases with increasing spanning molar mass, which limits the range of  $M_s$  for which the conformational relaxation can be determined reliably.

Figure 2 shows a comparison of the normalized dielectric loss spectra of linear PPO before and after end-linking, and Figure 3 shows this comparison for star PPO. All the spectra shown in Figures 2 and 3 were obtained at approximately  $T = T_g + 20$  K, and the contribution of the conductivity has been subtracted for clarity. From a mere visual inspection it is evident that there is no difference between the spectra of end-linked linear and star PPO if the spanning molar masses of the precursors are the same. This observation generalizes the findings in ref 15 for a range of molar masses and implies that the mobility of the chain segments

between the urethane bonds is the same in the entangled melt and in the gel.

The dielectric relaxation of the precursors was discussed in detail in ref 11. The main peak is due to the segmental relaxation and has a temperature dependence that is well described by the so-called Vogel–Fulcher equation:

$$\log(\tau_a) = \log(\tau_0) + \frac{B}{(T - T_0)} \quad (8)$$

The minor peak, which is clearly distinguished for the larger precursor, is due to fluctuations of the end-to-end vector of an arm, and its temperature dependence can also be described by the Vogel–Fulcher equation. The shape of both relaxation processes is independent of the temperature in the range covered. However, the

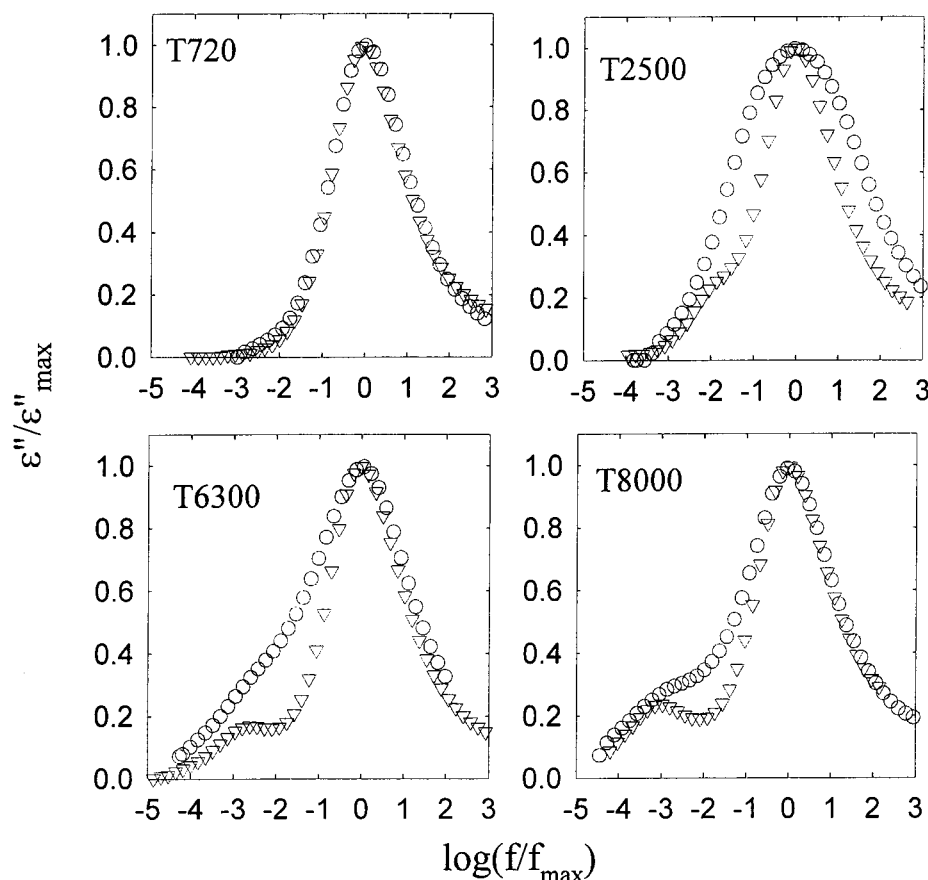


**Figure 3.** Comparison of the normalized dielectric loss spectra of star PPO before (triangles) and after (circles) end-linking.

slow mode has a weaker temperature dependence for  $T < T_g + 30$  K, and as a consequence the two modes merge if the temperature is lowered.

Figures 2 and 3 show that end-linking leads to broadening of the main peak for intermediate molar masses of the precursors. For very small and very large precursors the broadening is unimportant. The effect is similar to that observed in end-linked PPS,<sup>16</sup> and it has the same origin; i.e., the relaxation of a fraction of the PPO segments adjacent to the urethane links is slowed down. For low molar mass precursors the relaxation of the modified PPO segments dominates, while for high molar mass precursors the relaxation of the unmodified PPO segments dominates. It explains why the peak is relatively narrow at low and high molar masses. When both modes are significant, it leads to an apparent broadening of the peak, because the two modes are very close. For PPS the two modes could be clearly distinguished for  $M_s = 1.6$  kg/mol where they had approximately the same amplitude. For PPO the two modes cannot be distinguished, but the broadening is most important for approximately the same value of  $M_s$ . Of course, this picture of two distinct segment motions is only approximate as some segments will have an intermediate behavior.

Figure 4 shows the temperature dependence of the position of the dielectric loss peak of the end-linked diols. End-linked triols show a similar behavior. We plotted the data as a function of the reduced temperature ( $T - T_{gv}$ ), which removes the effect of different glass transition temperatures.  $T_{gv}$  is defined as the temperature where the loss peak of the shear modulus is situated at 1 rad/s.  $T_{gv}$  is close to  $T_g$  (see Table 1) but can be obtained with better precision. In this represen-

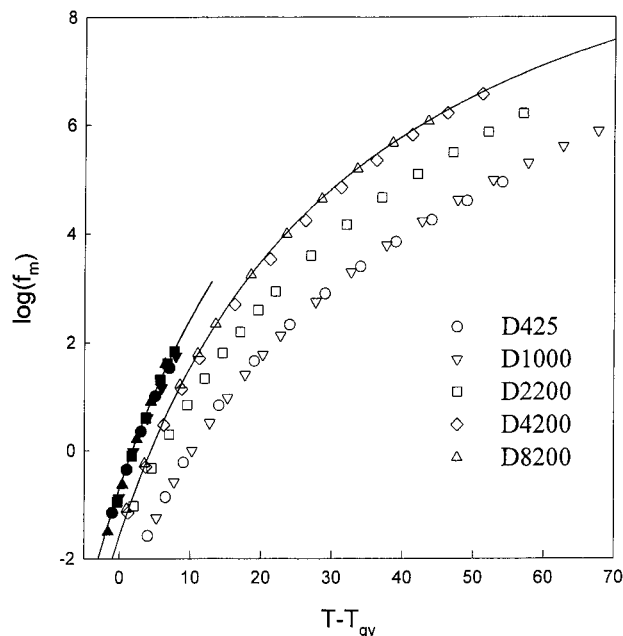


**Figure 4.** Reduced temperature dependence of the mechanical (filled symbols) and the dielectric (open symbols) loss peak of end-linked linear PPO with different molar masses. The solid lines represent the results obtained before end-linking.

tation all the precursors follow the same curve indicated by the solid line in Figure 4. For comparison, we also show the reduced temperature dependence of the loss peak of the shear modulus. Unfortunately, the mechanical loss peak can only be determined over a small range of temperatures due to the limited dynamical range of the rheometer. Over this range the reduced temperature



**Table 2. Glass Transition Temperatures of D425 at Different Connectivity Extents**

| $r$ | $T_g$ (K) | $T_{gv}$ | $r$ | $T_g$ (K) | $T_{gv}$ |
|-----|-----------|----------|-----|-----------|----------|
| 0   | 201       | 200      | 0.6 | 225       | 224      |
| 0.2 | 208       | 207      | 0.8 | 237       | 234      |
| 0.4 | 218       | 215      | 1.0 | 245       | 244      |

dependence of the mechanical loss peak is independent of the size of the precursors and is systematically situated at higher frequencies than the dielectric loss peak. It was found earlier for PPO and PPS with different molar masses that the difference is about a factor 10. The difference was attributed to the fact that the dielectric spectroscopy measures a compliance while the mechanical spectroscopy measures a modulus. If the relaxation is characterized by a distribution of relaxation times, the average relaxation time of a compliance is longer than that of a modulus. The same difference is observed here for large end-linked PPO. In fact, for large end-linked PPO the temperature dependence of the loss peaks is the same as that of the precursors and is characteristic for the relaxation of unmodified segments ( $\alpha$ -relaxation). However, a different reduced temperature dependence is found here for smaller precursors similar to that observed earlier for PPS. For small end-linked PPO one measures the relaxation of modified PPO segments ( $\alpha'$ -relaxation). Intermediate behavior is observed when the maximum position of the loss peak is influenced by both modes.

To investigate further the influence of end-linking on the segmental relaxation, I have measured the mechanical and dielectric relaxation of the smallest PPO diol (D425) as a function of the extent of end-linking ( $r$ ). This diol is too small to show a distinct relaxation of the end-to-end vector. The samples have been characterized using size exclusion chromatography, and the size distribution at different connectivity extents has been compared with mean field theory in ref 18.  $T_g$  determined with DSC is close to  $T_{gv}$  obtained from mechanical measurements (see Table 2) and increases approximately linearly with increasing  $r$ :  $T_g = 200 \text{ K} + 44r$ . As end effects on  $T_g$  are small for PPO due to hydrogen bonding, the increase of  $T_g$  is mainly caused by the incorporation of urethane groups. A similar dependence of  $T_g$  on  $r$  was reported earlier for the smallest PPO triol (T720).<sup>13</sup>

Figure 5a compares the dielectric loss peaks at various extents of end-linking. For comparison, we show the loss peaks of the shear modulus in Figure 5b. There is a striking difference between the  $r$  dependence of the half-width of the dielectric and the mechanical loss peaks (see Figure 6). The mechanical loss ( $G''$ ) peak broadens with increasing connectivity extent until  $r = 0.5$ , after which it stabilizes as was reported earlier for a small PPO triol.<sup>12</sup> However, the width of the dielectric loss peak has a maximum at  $r \approx 0.5$ , i.e., when half the hydroxyl groups have been replaced by urethane bonds. We did not observe a significant variation in the shape of the mechanical loss peaks in the temperature range covered by the experiment. However, the broadening of the dielectric loss peak increases slightly with decreasing temperature, i.e., with increasing  $f_{\text{max}}$ .

The influence of progressive end-linking on the dielectric relaxation of D425 corroborates the existence of two distinct relaxation modes: a faster  $\alpha$ -relaxation that is caused by the relaxation of unmodified PPO segments and a slower  $\alpha'$ -relaxation that is due to the relaxation of PPS segments modified by the urethane

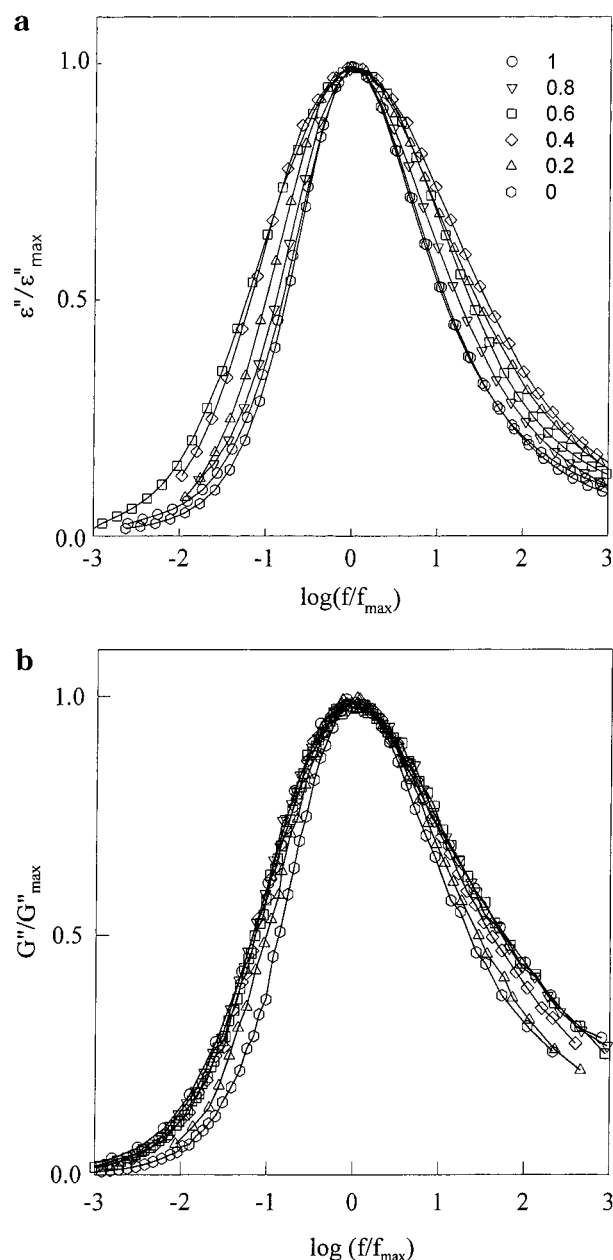


**Figure 5.** (a) Comparison of the normalized dielectric loss spectra of a small linear PPO (D425) at different connectivity extents ( $r$ ) indicated in the figure. (b) Comparison of the normalized mechanical loss spectra of a small linear PPO (D425) at different connectivity extents. The symbols are as in (a).

links. Each mode is relatively narrow and dominates at  $r$  close to 0 and close to 1, respectively. This explains the similarity of the peaks before and after end-linking for the smallest diol and triol (see Figure 2). The difference in the peak positions of each mode is not enough to show two distinct peaks but explains the broadening of the peak at intermediate values of  $r$ . Notice, however, that for this small sample the contribution of the hydroxyl end groups and the urethane links themselves may no longer be neglected. In fact, their contribution represents about half of the total dielectric permittivity. Nevertheless, the total signal varies little with  $r$ , which means that the signal from the hydroxyl groups is about the same as that from the urethane links. It follows that the  $\alpha$ -relaxation includes the relaxation of hydroxyl groups and the  $\alpha'$ -relaxation includes the relaxation of the urethane links.

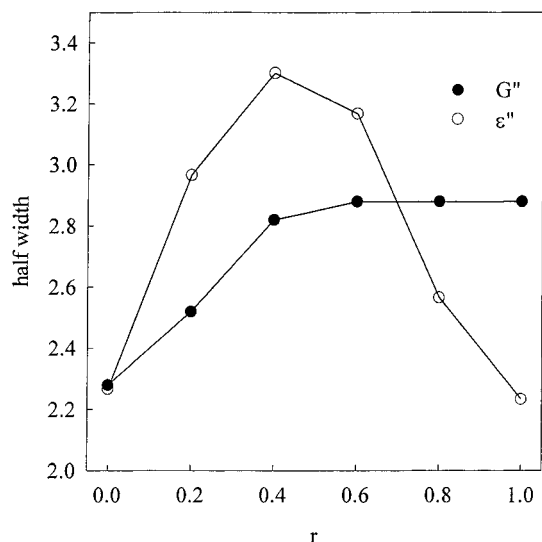


**Figure 6.** Comparison of the half-width of the dielectric and the mechanical loss peak ( $\Delta \log(f)$  at  $\epsilon'' = \epsilon''_{\max}/2$  or at  $G' = G'_{\max}/2$ ) as a function of the connectivity extent for a small linear PPO (D425).

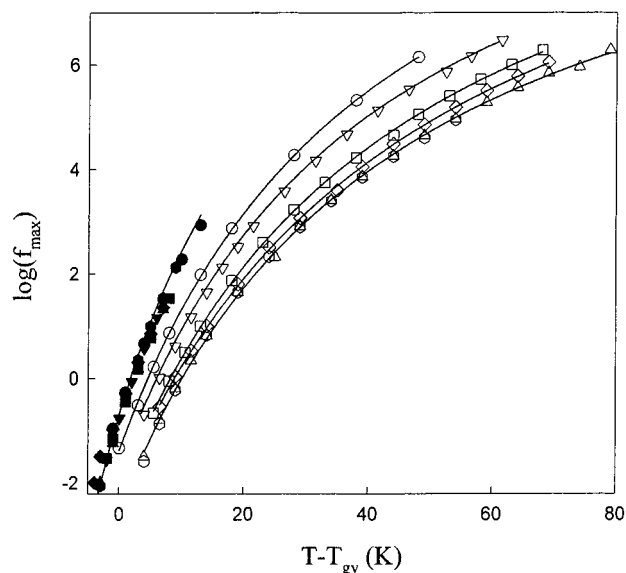


**Figure 7.** Reduced temperature dependence of the mechanical (filled symbols) and the dielectric (open symbols) loss peak of a small linear PPO (D425) at different connectivity extents. The symbols are as in Figure 5a. The solid lines represent fits to the Vogel-Fulcher equation.

The reduced temperature dependence of the position of the dielectric and mechanical loss peaks is shown in Figure 7. Again, the shear modulus loss peak is systematically situated at higher frequencies. The difference increases at larger  $r$  where the  $\alpha'$ -relaxation becomes dominant.

The present results obtained on a small PPO diol are very close to those obtained by Baillif et al.<sup>19</sup> in a DS study of small PPO triols. In one particular case they could distinguish the two relaxation modes using high-frequency DS. They also studied the effect of end-linking for one large PPO triol (T6300) which showed a weak progressive broadening with increasing  $r$ . This is expected as even at  $r = 1$  the fraction of modified PPO segments is small.

It appears that the main loss peak of the dielectric permittivity of polyurethane can be explained in terms

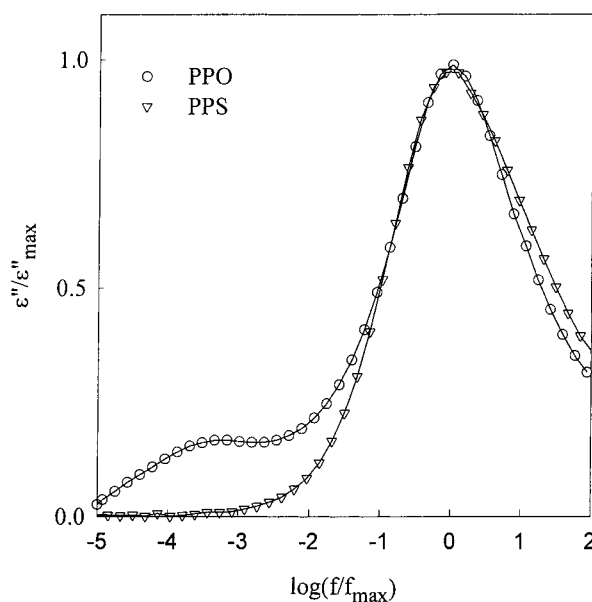


**Figure 8.** Comparison of the dielectric loss of end-linked PPO (D8200) and end-linked PPS with approximately the same number of segments ( $\pm 80$ ). The reference temperature is  $T_{gv} + 20$  K.

of two relaxation processes: that of PPO segments modified by the urethane links and of PPO segments that are far enough removed not to be influenced. The  $\alpha'$ -relaxation is not so obvious in the loss peak of the shear modulus, although the broadening of the loss peak in polyurethane with a high density of urethane links might point to its influence. PPS does not have a significant dipole moment parallel to the main chain but does show the same effects on the main dielectric loss peak after end-linking with the same diisocyanate. The comparison between the two polymers shows that the main loss peak is solely due to the relaxation of the dipole moment perpendicular to the main chain (see Figure 8).

The influence of end-linking on the relaxation of the dipole moment parallel to the main chain, i.e., of the end-to-end vector, can only be seen clearly if large precursors are used. For smaller precursors this relaxation is obscured by the broadening of the main peak. The low-frequency end of the loss peaks shown in Figures 2 and 3, which is least influenced by the main relaxation, is remarkably close to that of the precursors. This observation implies that the relaxation of the end-to-end vector of the PPO chains is not much influenced after they become part of long entangled chains or a system spanning network. We note that the dipole moment is inverted at the center of the PPO chain as well as at the urethane links, which means that DS probes the relaxation of a single arm, taking PPO diol as a star with two arms.

For all systems investigated here the molar mass of the PPO arms is smaller than or close to the entanglement molar mass. It is thus not surprising that the end-to-end vector relaxation of the PPO arms is not much influenced in linear polyurethane. After all, the Rouse model assumes that the relaxation of the end-to-end vector of part of a chain is independent of movement on a larger length scale as long as it is not entangled. The experimental results on cross-linked polyurethane show that the so-called phantom model of gel elasticity is more realistic than the so-called affine model for these

gels. The former model assumes that the cross-links are fully mobile over the average distance between cross-links while the latter assumes that their mobility is restricted.<sup>20</sup>

### Conclusion

There is no difference between the dielectric relaxation of linear and cross-linked polyurethane with the same density of urethane bonds. The relaxation of the end-to-end vector of the chain backbone is not significantly modified by end-linking at least if they are not entangled. The dielectric relaxation of the dipole moment perpendicular to the chain backbone is modified by the presence of urethane bonds. The effect is the same as reported earlier for PPS and may be interpreted in terms of more restricted movement of a number of segments close to the urethane links.

### References and Notes

- (1) Schönhals, A.; Schlosser, E. *Phys. Scr.* **1993**, T49, 233.
- (2) Schlosser, E.; Schönhals, A. *Prog. Colloid Polym. Sci.* **1993**, 91, 158.
- (3) Bauer, M. E.; Stockmayer, W. H. *J. Chem. Phys.* **1965**, 43, 4319.
- (4) Stockmayer, W. H.; Bauer, M. E. *Macromolecules* **1969**, 2, 647.
- (5) Yano, S.; Rabalkar, R. R.; Hunter, S. P.; Wang, C. H.; Boyd, R. H. *J. Polym. Sci., Polym. Phys. Ed.* **1976**, 14, 1877.
- (6) Cochrane, J.; Harrison, G.; Lamb, J.; Phillips, D. W. *Polymer* **1980**, 21, 837.
- (7) Alper, T.; Barlow, A. J.; Gray, R. W. *Polymer* **1976**, 17, 665.
- (8) Johari, G. P. *Polymer* **1986**, 27, 866.
- (9) Randriantoandro, H.; Nicolai, T. *Macromolecules* **1997**, 30, 2460.
- (10) Nicolai, T.; Floudas, G. *Macromolecules* **1998**, 31, 2578.
- (11) Nicolai, T.; Prochazka, F.; Durand, D. *J. Rheol.* **1999**, 43, 1511.
- (12) Prochazka, F.; Nicolai, T.; Durand, D. *Macromolecules* **1996**, 29, 2260.
- (13) Randrianantoandro, H.; Nicolai, T.; Prochazka, F.; Durand, D. *Macromolecules* **1997**, 30, 5893.
- (14) Nicolai, T.; Randrianantoandro, H.; Prochazka, F.; Durand, D. *Macromolecules* **1997**, 30, 5897.
- (15) Nicolai, T.; Prochazka, F.; Durand, D. *Phys. Rev. Lett.* **1999**, 82, 863.
- (16) Nicol, E.; Nicolai, T.; Durand, D. *Macromolecules* **1999**, 32, 5893.
- (17) Nicol, E.; Nicolai, T.; Durand, D. *Macromolecules* **2001**, 34, 59.
- (18) Prochazka, F.; Nicolai, T.; Durand, D. *Macromolecules* **2000**, 33, 1703.
- (19) Baillif, P.; Tabellout, M.; Emery, J. R. *Polymer* **2000**, 41, 5305.
- (20) Mark, J. E.; Erman, B. *Rubberlike Elasticity a Molecular Primer*; John Wiley and Sons: New York, 1988.

MA011005Z